1

Electro-Optic Effect

The electro-optic effect together with photoconductivity are the fundamental phenomena underlying the photorefractive effect. Most photorefractive crystals are anisotropic (their properties are different along different directions) and even those that are not become anisotropic under the action of an externally applied electric field. So, we shall start with a review of light propagation in anisotropic media. These materials usually exhibit piezoelectric effects too [1–3] but, for the sake of simplicity, we shall not consider them here.

The electro-optic effect in photorefractive materials is of the highest importance because it is at the origin of the "imaging" of a space-charge field modulation into an index-of-refraction modulation; that is to say, a volume grating. In fact, the build up of a holographic grating in photorefractive materials consists of the spatial modulation of the index-of-refraction in the volume of the sample. In these materials, such a modulation arises from the build-up of a modulated space-charge field that on its turn modulates the index-of-refraction via an electro-optic effect.

1.1 Light Propagation in Crystals

Crystals are, in general, anisotropic, that is to say, they have different properties for the light propagating along different directions.

1.1.1 Wave Propagation in Anisotropic Media

Let us start with the general vectorial relations

$$\vec{D} = \epsilon_o \vec{E} + \vec{P} \tag{1.1}$$

$$\vec{P} = \epsilon_o \hat{\chi} \vec{E} \tag{1.2}$$

where $\epsilon_0 = 8.82 \times 10^{-12}$ coul/(mV) is the permittivity of vacuum. The quantities $\vec{P}$, $\vec{E}$ and $\vec{D}$ are the polarization, electric field and displacement fields, respectively, with $\hat{\chi}$ (polarizability) being a tensor that, for isotropic media only, can be written as a scalar thus simplifying the relation in Eq. (1.2)

$$\vec{P} = \epsilon_o \chi \vec{E} \tag{1.3}$$

The relation in Eq. (1.2) can also be written as

$$\begin{bmatrix} P_1 \\ P_2 \\ P_3 \end{bmatrix} = \epsilon_o \begin{bmatrix} \chi_{11} & \chi_{12} & \chi_{13} \\ \chi_{21} & \chi_{22} & \chi_{23} \\ \chi_{31} & \chi_{32} & \chi_{33} \end{bmatrix} \begin{bmatrix} E_1 \\ E_2 \\ E_3 \end{bmatrix} \tag{1.4}$$

Photorefractive Materials for Dynamic Optical Recording: Fundamentals, Characterization, and Technology, First Edition. Jaime Frejlich.

and also

$$\vec{D} = \varepsilon_o(\hat{1} + \hat{\chi})\vec{E} \tag{1.5}$$

where $\hat{1}$ and $\hat{\chi}$ are tensors that are written as:

$$\hat{1} = \begin{bmatrix} 1 & 0 & 0 \\ 0 & 1 & 0 \\ 0 & 0 & 1 \end{bmatrix} \qquad \hat{\chi} = \begin{bmatrix} \chi_{11} & \chi_{12} & \chi_{13} \\ \chi_{21} & \chi_{22} & \chi_{23} \\ \chi_{31} & \chi_{32} & \chi_{33} \end{bmatrix} \tag{1.6}$$

Let us recall that there is always a set of coordinate axes, called "principal axes" where $\hat{\chi}$ assumes a diagonal form

$$\hat{\chi} = \begin{bmatrix} \chi_{11} & 0 & 0 \\ 0 & \chi_{22} & 0 \\ 0 & 0 & \chi_{33} \end{bmatrix} \tag{1.7}$$

1.1.2 General Wave Equation

The equation describing the electromagnetic wave in nonmagnetic and noncharged media can be deduced from Maxwell's equations

$$\nabla \times \vec{E} = -\mu_o \frac{\partial \vec{H}}{\partial t} \tag{1.8}$$

$$\nabla \times \vec{H} = \varepsilon_o \frac{\partial \vec{E}}{\partial t} + \frac{\partial \vec{P}}{\partial t} + \vec{J} \quad \text{with} \quad \vec{J} = \sigma \vec{E} \tag{1.9}$$

$$\nabla . \vec{E} = -\frac{1}{\varepsilon_o} \nabla . \vec{P} \tag{1.10}$$

$$\nabla . \vec{H} = 0 \tag{1.11}$$

In a system of principal coordinate axes, it is

$$\begin{array}{lll} P_1 = \varepsilon_o \chi_{11} E_1 & D_1 = \varepsilon_{11} E_1 & \varepsilon_{11} = \varepsilon_o(1 + \chi_{11}) \\ P_2 = \varepsilon_o \chi_{22} E_2 & D_2 = \varepsilon_{22} E_2 & \varepsilon_{22} = \varepsilon_o(1 + \chi_{22}) \\ P_3 = \varepsilon_o \chi_{33} E_3 & D_3 = \varepsilon_{33} E_3 & \varepsilon_{33} = \varepsilon_o(1 + \chi_{33}) \end{array} \tag{1.12}$$

1.1.3 Index Ellipsoid

We shall write the expressions for the electric w_e and magnetic w_m energy densities in electromagnetic waves as [4]

$$w_e = \frac{1}{2}\vec{E} . \vec{D} = \frac{1}{2} \sum_{kl} E_k \epsilon_{kl} E_l \qquad w_m = \frac{1}{2}\vec{B} . \vec{H} = \frac{1}{2}\mu H^2 \tag{1.13}$$

and write the Poynting formulation for the energy flux as

$$\vec{S} = \vec{E} X \vec{H} \tag{1.14}$$

After adequate substitutions and transformations taking into account Maxwell's equations, for the principal coordinate axes we get

$$\frac{D_x^2}{\epsilon_x} + \frac{D_y^2}{\epsilon_y} + \frac{D_z^2}{\epsilon_z} = 8\varepsilon_o \pi w_e = \text{constant} \qquad \begin{array}{l} \epsilon_x \equiv \epsilon_{11} = 1 + \chi_{11} \\ \epsilon_y \equiv \epsilon_{22} = 1 + \chi_{22} \\ \epsilon_z \equiv \epsilon_{33} = 1 + \chi_{33} \end{array} \tag{1.15}$$

Following the definitions

$$x = \frac{D_x}{\sqrt{w_e \varepsilon_o}}$$
$$y = \frac{D_y}{\sqrt{w_e \varepsilon_o}}$$
$$z = \frac{D_z}{\sqrt{w_e \varepsilon_o}}$$

with

$$n_x^2 = \epsilon_x = \varepsilon_x / \varepsilon_o$$
$$n_y^2 = \epsilon_y = \varepsilon_y / \varepsilon_o$$
$$n_z^2 = \epsilon_z = \varepsilon_z / \varepsilon_o$$

we get the indicatrix formulation

$$\frac{x^2}{n_x^2} + \frac{y^2}{n_y^2} + \frac{z^2}{n_z^2} = 1 \tag{1.16}$$

where n_x, n_y and n_z are the index-of-refraction along coordinates x, y and z, respectively, as represented in Fig. 1.1. In order to use this ellipsoid to analyze the propagation of a plane wave with propagation vector $\vec{k}$, we just intersect the indicatrix with a plane orthogonal to the vector $\vec{k}$. An elliptic figure results where the extraordinary n_e and ordinary n_o indexes for this wave are found from the intersection with the corresponding direction of vibration of the electric field, as shown in Fig. 1.2. In the next section, we shall analyze Eq. (1.16) in a more general form.

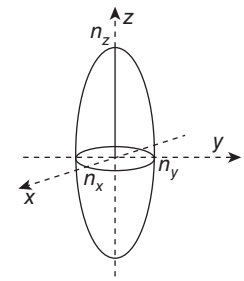

Figure 1.1 Refractive index ellipsoid.

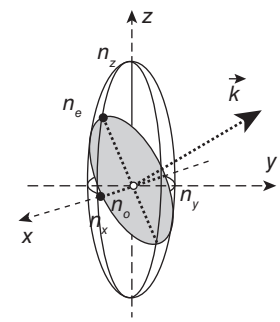

Figure 1.2 Refractive indices for a plane wave propagating in an anisotropic medium.

1.2 Tensorial Analysis

Let us write the general equation [5]

$$\sum_{i=1,j=1}^{i=N,j=N} S_{ij}x_i x_j = 1 \text{ or } S_{i,j}x_i x_j = 1 \tag{1.17}$$

where x_i and x_j are variables and S_{ij} are coefficients. If we assume that $S_{ij} = S_{ji}$, then Eq. (1.17) turns into the general ellipsoid representation:

$$S_{11}x_1^2 + S_{22}x_2^2 + S_{33}x_3^2 + 2S_{12}x_1x_2 + 2S_{13}x_1x_3 + 2S_{23}x_2x_3 = 1 \tag{1.18}$$

Equation (1.18) can be transformed into new coordinate axes x_i', by using the axes-transformation matrix, as follows

$$\begin{aligned} x_1' &= a_{11}x_1 + a_{12}x_2 + a_{13}x_3 \\ x_2' &= a_{21}x_1 + a_{22}x_2 + a_{23}x_3 \\ x_3' &= a_{31}x_1 + a_{32}x_2 + a_{33}x_3 \end{aligned} \tag{1.19}$$

that can be written in a matricial form

$$\begin{bmatrix} x_1' \\ x_2' \\ x_3' \end{bmatrix} = \begin{bmatrix} a_{11} & a_{12} & a_{13} \\ a_{21} & a_{22} & a_{23} \\ a_{31} & a_{32} & a_{33} \end{bmatrix} \begin{bmatrix} x_1 \\ x_2 \\ x_3 \end{bmatrix} \tag{1.20}$$

From the matricial relation (1.20), we should deduce that it is also

$$\begin{bmatrix} x_1 \\ x_2 \\ x_3 \end{bmatrix} = \begin{bmatrix} a_{11} & a_{21} & a_{31} \\ a_{12} & a_{22} & a_{32} \\ a_{13} & a_{23} & a_{33} \end{bmatrix} \begin{bmatrix} x_1' \\ x_2' \\ x_3' \end{bmatrix} \tag{1.21}$$

The relation in Eq. (1.20) can be written in the form

$$x_i = a_{ki}x_k' \qquad x_j = a_{lj}x_l' \tag{1.22}$$

that substituted into Eq. (1.18) leads to

$$S_{ij}x_i x_j = S_{ij}a_{ki}a_{lj}x_k'x_l' = S_{kl}'x_k'x_l' \tag{1.23}$$

where S_{kl}' are the coefficients in the new coordinate system. An ellipsoid can be used to describe any symmetric tensor ($S_{ij} = S_{ji}$) of second order, and is especially useful to describe any property in a crystal that should be represented by a tensor. An important property of an ellipsoid is the presence of "principal axes", in which case Eq. (1.18) can be simplified to

$$S_{11}x_1^2 + S_{22}x_2^2 + S_{33}x_3^2 = 1 \qquad \Rightarrow \qquad S_{ij} = \begin{bmatrix} S_{11} & 0 & 0 \\ 0 & S_{22} & 0 \\ 0 & 0 & S_{33} \end{bmatrix} \tag{1.24}$$

1.3 Electro-Optic Effect

The indicatrix in Eq. (1.16) is an ellipsoid in a principal coordinate axes system. Its general formulation is [5]

$$B_{ij}x_i x_j = 1 \quad \text{with} \quad B_{ij} = \frac{1}{\epsilon_{ij}} \tag{1.25}$$

The slight variation in the refractive index produced by an electric field can be described by the third-order electro-optic tensor r_{ijk} (in the range of 10^{-12} m/V for most materials) through the relation

$$\Delta B_{ij} = r_{ijk} E_k \tag{1.26}$$

$$\text{From } B_{ij} = B_{ji} \qquad \Rightarrow \qquad r_{ijk} = r_{jik} \tag{1.27}$$

The B-tensor can be written as

$$\begin{bmatrix} B_{11} & B_{12} & B_{13} \\ B_{21} & B_{22} & B_{23} \\ B_{31} & B_{32} & B_{33} \end{bmatrix} = \begin{bmatrix} B_1 & B_6 & B_5 \\ B_6 & B_2 & B_4 \\ B_5 & B_4 & B_3 \end{bmatrix} \tag{1.28}$$

The electro-optic relation is therefore simplified to

$$\Delta B_i = r_{ij} E_j \qquad (i = 1, 2, 3, 4, 5, 6; j = 1, 2, 3) \tag{1.29}$$

or explicitly written as

$$\begin{bmatrix} \Delta B_1 \\ \Delta B_2 \\ \Delta B_3 \\ \dots \\ \Delta B_6 \end{bmatrix} = \begin{bmatrix} r_{11} & r_{12} & r_{13} \\ r_{21} & r_{22} & r_{23} \\ r_{31} & r_{32} & r_{33} \\ \dots & \dots & \dots \\ r_{61} & r_{62} & r_{63} \end{bmatrix} \begin{bmatrix} \Delta E_1 \\ \Delta E_2 \\ \Delta E_3 \end{bmatrix} \tag{1.30}$$

Let us assume that an electric field is applied, with components E_1, E_2, E_3 as represented in Fig. 1.3 for a sillenite crystal so that Eq. (1.25) turns into:

$$\begin{aligned} &(B_1 + r_{11}E_1 + r_{12}E_2 + r_{13}E_3)x_1^2 + \\ &(B_2 + r_{21}E_1 + r_{22}E_2 + r_{23}E_3)x_2^2 + \\ &(B_3 + r_{31}E_1 + r_{32}E_2 + r_{33}E_3)x_3^2 + \\ &(B_4 + 2r_{41}E_1 + 2r_{42}E_2 + 2r_{43}E_3)x_2x_3 + \\ &(B_5 + 2r_{51}E_1 + 2r_{52}E_2 + 2r_{53}E_3)x_1x_3 + \\ &(B_6 + 2r_{61}E_1 + 2r_{62}E_2 + 2r_{63}E_3)x_1x_2 = 1 \end{aligned} \tag{1.31}$$

We are interested in the slow index-of-refraction build up produced by the slow accumulation of electric charges. Therefore, all the electro-optic coefficients referred to in this chapter are only the low-frequency ones only. In the following sections, we shall see what Eq. (1.31) looks like for some particular materials.

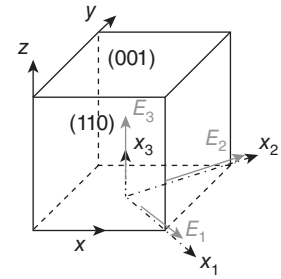

Figure 1.3 Crystallographic axes of a sillenite and an applied 3D electric field.

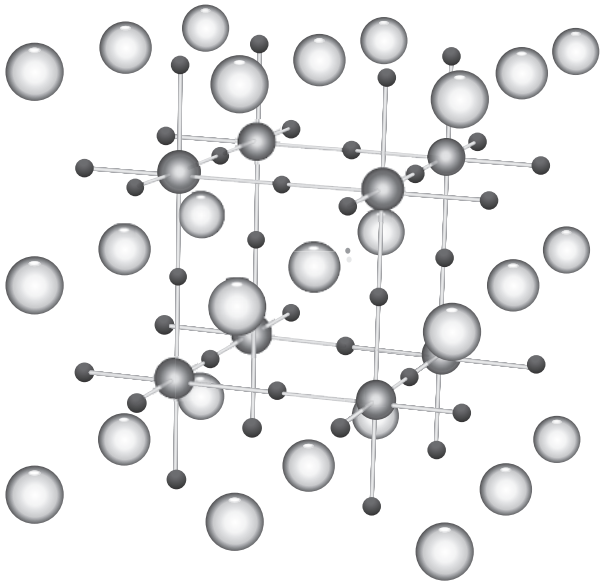

Figure 1.4 Structure of an undistorted cubic perovskite structure with general chemical formula ABX_3. The differently shaded spheres represent X atoms (usually oxygens), B atoms (a smaller metal cation, such as Ti^{4+}) and A atoms (a larger metal cation, such as Ca^{2+}).

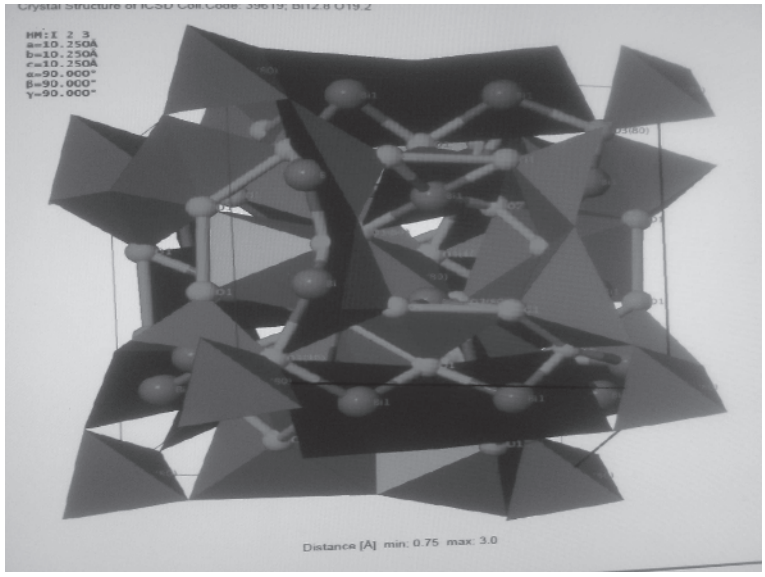

Figure 1.5 Three-dimensional sillenite structure: darker spheres represent Bi^{3+} ions and paler gray ones are O^{2-}. Acknowledgments to Prof. Jesiel F. Carvalho, IF/UFG-Goiânia-GO, Brazil.

1.4 Perovskite Crystals

Calcium titanium oxide ($CaTiO_3$) is a typical representative of the Perovskite crystal structure. The general chemical formula is ABX_3, where "A" and "B" are two cations of very different sizes, and "X" is an anion (usually O) that bonds to both (see Fig. 1.4). The "A" atoms are larger than the "B" atoms and the latter is in six-fold coordination, surrounded by an octahedron of anions, and the "A" cation in 12-fold cuboctahedral coordination. Perovskites are the best-known and the largest family of ferroelectric and piezoelectric materials, such as single crystals of $BaTiO_3$, $PbTiO_3$, Pb(Zr, Ti)O_3 and $KNbO_3$.

1.5 Sillenite Crystals

Sillenites are cubic crystal structures with general chemical formula $Bi_{12}MO_{20}$ where M=Si, Ti,Ge,Ga (see Fig. 1.5). The well-known crystals of this family are: $Bi_{12}GeO_{20}$ (BGO),$Bi_{12}GaO_{20}$ (BGaO), $Bi_{12}SiO_{20}$ (BSO), and $Bi_{12}TiO_{20}$ (BTO). They belong to the cubic noncentrosymmetric crystal point class 23 and are piezo-electric, electro- and elasto-optic, optically active and usually photoconductive.

BTO is the crystal with the lowest optical activity (optical activity is undesirable for most applications) but is also the most difficult to grow because the chemical composition of the melt and the crystal are different, they are noncongruent. These crystals are usually grown using the so-called "top seed solution growth" $(TSSG)_{20}$.

The axes in the sample are conveniently renamed, accounting for its cubic and isotropic nature in which case the axes [001], [010] and [100], for example, can be interchanged. In the slanted-sliced sample in Fig. 1.6, the striations are not visible through the polished (110)-face (see also Figs 1.7 and 1.8).

The electro-optic tensor of this crystal family in the principal-axes coordinates $[X_1, X_2, X_3]$ has the following elements [7]:

$$r_{41} = r_{52} = r_{63} \approx 5 \times 10^{-12}\ \mathrm{m/V} \tag{1.32}$$

all other elements being zero.

1.5.1 Index Ellipsoid

In the absence of electric field ($E = 0$), the index ellipsoid is

$$\frac{x_1^2 + x_2^2 + x_3^2}{n_o^2} = 1 \tag{1.33}$$

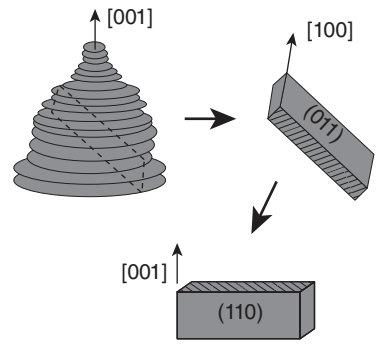

Figure 1.6 Schematic representation of a raw BTO crystal boule with its striations, indicating the way it will be sliced (top left); already sliced crystal with striations not perpendicular to the (011)-face (top right) and ready-to-use crystal with renamed axes (bottom).

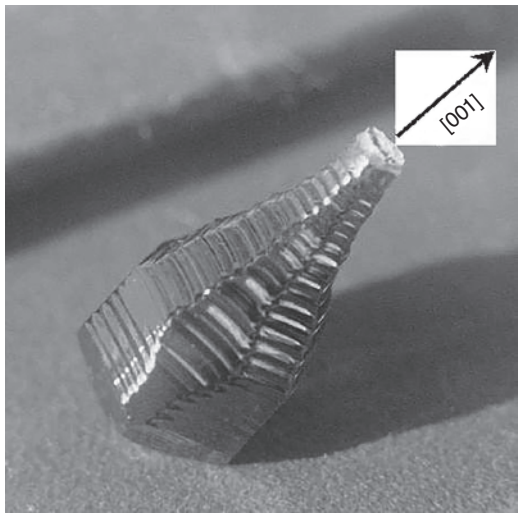

Figure 1.7 $Bi_{12}TiO_{20}$ crystal boule as grown along its [001]-axis.

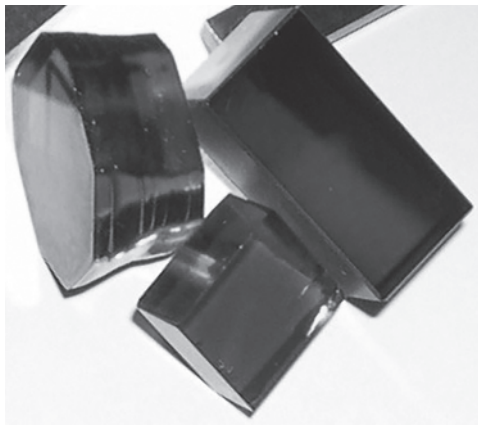

Figure 1.8 Actual undoped sillenite crystals: raw $Bi_{12}TiO_{20}$ crystal boule grown along its [001]-axis, showing striations on the lateral surfaces with both opposite (001)-faces cut and polished (left); $Bi_{12}SiO_{20}$ crystal showing its (110)-surface cut and polished (center) and $Bi_{12}TiO_{20}$ crystal with its larger (110)-face cut and polished with its [001]-axis direction along its longer dimension (right).

showing that we are dealing with an isotropic crystal. Applying an electric field along direction "x" as indicated in Fig. 1.10, we have the field components:

$$E_1 = E_2 = E\frac{\sqrt{2}}{2} \qquad E_3 = 0 \tag{1.34}$$

so that the index ellipsoid is modified to:

$$\frac{x_1^2}{n_o^2} + \frac{x_2^2}{n_o^2} + \frac{x_3^2}{n_o^2} + 2r_{41}E_1x_2x_3 + 2r_{52}E_2x_1x_3 = 1 \tag{1.35}$$

or

$$\frac{x_1^2}{n_o^2} + \frac{x_2^2}{n_o^2} + \frac{x_3^2}{n_o^2} + 2r_{41}E\frac{\sqrt{2}}{2}(x_2x_3 + x_1x_3) = 1 \tag{1.36}$$

Let us now rotate the system from coordinates X_1, X_2, X_3 to coordinates X, Y, Z in Fig. 1.10:

$$x = (x_1 + x_2)\frac{\sqrt{2}}{2} \tag{1.37}$$

$$y = (x_2 - x_1)\frac{\sqrt{2}}{2} \tag{1.38}$$

$$z = x_3 \tag{1.39}$$

which, when substituted into Eq. (1.36) and rearranged gives

$$\frac{x^2}{n_o^2} + \frac{y^2}{n_o^2} + \frac{z^2}{n_o^2} + 2r_{41}E\,x\,z = 1 \tag{1.40}$$

To eliminate this term in "*xz*" it is necessary to carry out another rotation, now in the "*x–z*" plane as shown in Fig 1.11

$$x = (\eta + \zeta)\frac{\sqrt{2}}{2} \tag{1.41}$$

$$z = (\eta - \zeta)\frac{\sqrt{2}}{2} \tag{1.42}$$

which, when substituted into Eq. (1.40) gives the relation

$$\zeta^2\left(\frac{1}{n_o^2} - r_{41}E\right) + \eta^2\left(\frac{1}{n_o^2} + r_{41}E\right) + \frac{y^2}{n_o^2} = 1 \tag{1.43}$$

which means that the refractive indices along the new axes ζ, η and y are:

$$n_\zeta = n_o + \frac{1}{2}n_o^3 r_{41}E \tag{1.44}$$

$$n_\eta = n_o - \frac{1}{2}n_o^3 r_{41}E \tag{1.45}$$

$$n_y = n_o \tag{1.46}$$

for $n_o \gg n_o^3 r_{41}E/2$. The wavelength dependence of n_o is reported in Fig. 1.9.

1.5.1.1 Index Ellipsoid with Applied Electric Field

Following the mathematical development here, it is possible to show that, for an electric field $\vec{E}$ along the axis [001], as shown in Fig. 1.12, the principal axes of the index ellipsoid are

$$x^2\left(\frac{1}{n_0^2} + r_{63}E\right) + y^2\left(\frac{1}{n_0^2} - r_{63}E\right) + \frac{z^2}{n_0^2} = 1 \tag{1.47}$$

with its principal axes directed along *x*, *y* and *z* and the corresponding indexes of refraction being:

$$n_x = n_0 - \frac{1}{2}n_0^3 r_{63}E \tag{1.48}$$

$$n_y = n_0 + \frac{1}{2}n_0^3 r_{63}E \tag{1.49}$$

$$n_z = n_0 \tag{1.50}$$

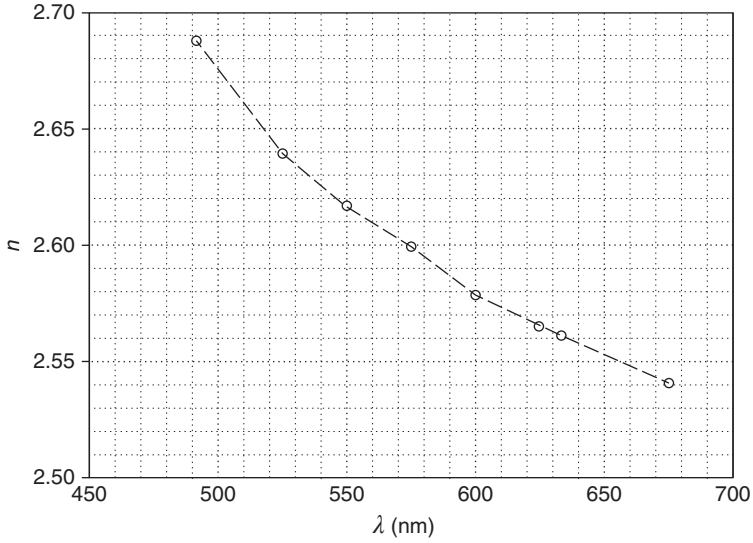

Figure 1.9 Index-of-refraction of BTO that is formulated by $n = 0.00863/\lambda^4 + 0.0199/\lambda^2 + 2.46$ [6].

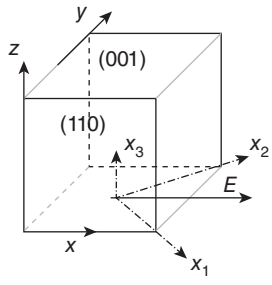

Figure 1.10 $Bi_{12}SiO_{20}$-type cubic crystal and its crystallographic axes X_1, X_2 and X_3 with an externally electric field E applied along the "x"-direction.

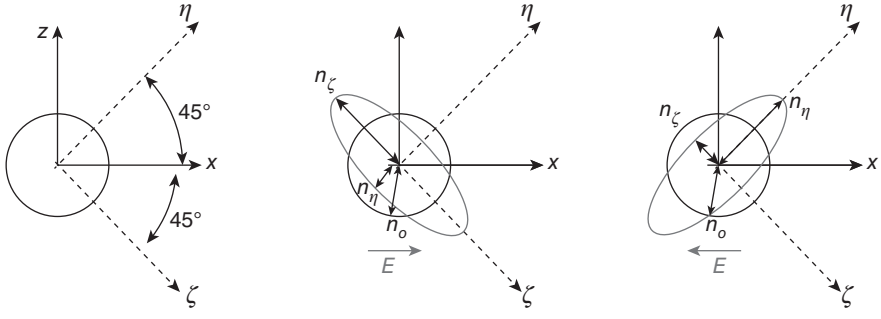

Figure 1.11 Principal coordinate axes system $\eta - \zeta$ arising by the effect of an electric field E applied along the "x"-axis, as shown in Fig. 1.10.

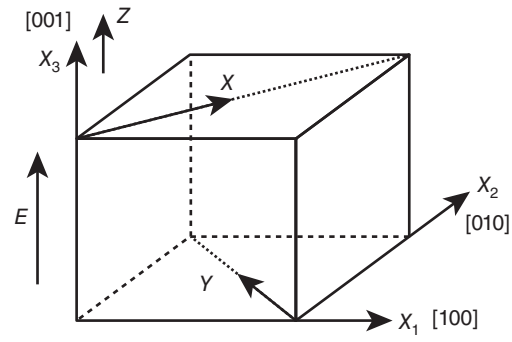

Figure 1.12 Sillenite crystal cut along its principal crystallographic axes, with an electric field along the [001]-axis.

thus meaning that, in the input crystal plane (110) that is also the x–z plane, the index of refraction changes only along x and is constant along z.

If the sillenite crystal is cut along its principal axes as shown in Fig. 1.12, with the (X_1, X_3) being the input plane, and the electric field $\vec{E}$ always along axis [001], it will produce index-of-refraction variations only in the (X_1, X_2) plane but nothing in the input plane (X_1, X_3). That is the reason why, for practical applications, these crystals should be cut as in Fig. 1.10 and not along its crystallographic axes as in Fig. 1.12.

1.5.2 Other Cubic Noncentrosymmetric Crystals

GaAs, InP and CdTe are also cubic noncentrosymmetric crystals, though they belong to the point class $\bar{4}3m$ but have the same electro-optic tensor structure as sillenites, that is to say that all elements are zero except

$$r_{41} = r_{52} = r_{63} = 1.72 \text{ pm V}^{-1} \quad \text{for GaAs} \tag{1.51}$$

$$r_{41} = r_{52} = r_{63} = 1.34 \text{ pm V}^{-1} \quad \text{for InP} \tag{1.52}$$

$$r_{41} = r_{52} = r_{63} = 5.5 \text{ pm V}^{-1} \quad \text{for CdTe} \tag{1.53}$$

The $\bar{4}$3m symmetry, however, guarantees that there is no optical activity. The index-of-refraction of CdTe varies from 2.86 at $\lambda = 1.06$ μm to 2.73 at $\lambda = 1.55$ μm and follows the relation [8]:

$$n^2 = 4.744 + \frac{2.424\lambda^2}{\lambda^2 - 282181.61} \tag{1.54}$$

1.5.3 Lithium Niobate

$LiNbO_3$ is a ferroelectric material [9] the structure of which, in principle, can be described as a highly distorted perovskite structure, to which it can be related by a displacive transformation. The $LiNbO_3$ structure is often considered as a distinct structure type from perovskites because small A cations have octahedral six-fold coordination instead of a 7–12-fold coordination in perovskites [10].

The electro-optic tensor, in the principal axes system $[X_1, X_2, X_3]$ for this material, has zero elements everywhere except the following ones [11]:

$$r_{12} = -r_{22} = r_{61} \approx 6.8 \text{ pm/V} \tag{1.55}$$

$$r_{13} = r_{23} = 10.0 \text{ pm/V} \qquad r_{33} = 32.2 \text{ pm/V} \qquad r_{42} = r_{51} = 32 \text{ pm/V} \tag{1.56}$$

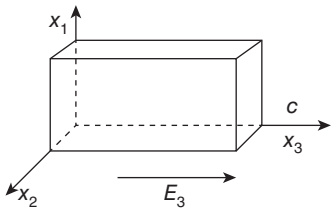

Figure 1.13 Lithium niobate crystal with an applied electric field along the photovoltaic *c*-axis.

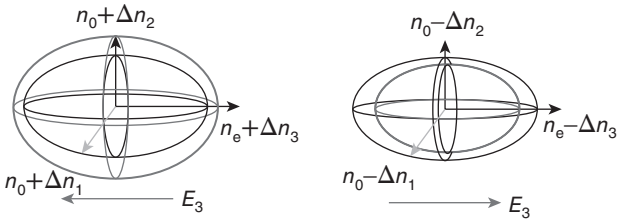

Figure 1.14 Lithium niobate crystal ellipsoid (black) and its modified (gray) size by the action of an applied field in opposite directions (left and right pictures) along the *c*-axis.

For an electric field E_3 applied along axis x_3 as shown in Fig. 1.13, the tensorial equation Eq. (1.31) becomes:

$$\left(\frac{1}{n_o^2}+r_{13}E_3\right)x_1^2+\left(\frac{1}{n_o^2}+r_{13}E_3\right)x_2^2+\left(\frac{1}{n_e^2}+r_{33}E_3\right)x_3^2=1 \tag{1.57}$$

with $n_o = 2.286$ and $n_e = 2.200$ at $\lambda = 633$ nm [1] and the following relations

$$\Delta\left(\frac{1}{n_1^2}\right)=-2\frac{1}{n_o^3}\Delta(n_1)=r_{13}E_3 \Rightarrow \Delta(n_1)=-\frac{n_o^3}{2}r_{13}E_3 \tag{1.58}$$

$$\Delta\left(\frac{1}{n_2^2}\right)=-2\frac{1}{n_o^3}\Delta(n_2)=r_{13}E_3 \Rightarrow \Delta(n_2)=-\frac{n_o^3}{2}r_{13}E_3 \tag{1.59}$$

$$\Delta\left(\frac{1}{n_3^2}\right)=-2\frac{1}{n_e^3}\Delta(n_3)=r_{33}E_3 \Rightarrow \Delta(n_3)=-\frac{n_e^3}{2}r_{33}E_3 \tag{1.60}$$

and the index-ellipsoid is modified as shown in Fig. 1.14.

1.5.4 KDP-(KH_2PO_4)

This crystal is actually not a photorefractive one but is here included as an example of electro-optic tensor somewhat similar to that of sillenites. It has the following electro-optic tensor:

$$r_{ij}=\begin{bmatrix}0&0&0\\0&0&0\\0&0&0\\r_{41}&0&0\\0&r_{52}&0\\0&0&r_{63}\end{bmatrix} \qquad r_{41}=r_{52}=8.6\ \text{pm/V} \qquad r_{63}=10.6\ \text{pm/V} \tag{1.61}$$

The index-of-refraction for this material is reported in Table 1.1.

Table 1.1 Index of refraction of KDP.

λ (nm)	n_o	n_e
546	1.5115	1.4698
633	1.5074	1.4669

The indicatrix equation formulated in the principal coordinate (crystallographic) axes X_1, X_2 and X_3, as represented in Fig. 1.10, is

$$\frac{x_1^2}{n_o^2} + \frac{x_2^2}{n_o^2} + \frac{x_3^2}{n_e^2} + 2r_{41}\, E_1\, x_2\, x_3 + 2r_{52}\, E_2\, x_1\, x_3 + 2r_{63}\, E_3\, x_1\, x_2 = 1 \tag{1.62}$$

Le us assume an externally applied field E_3 along the axis x_3 only. In this case we should proceed as for the case of $Bi_{12}SiO_{20}$ in Fig. 1.11 in order to get the following ellipsoid

$$\zeta^2 \left(\frac{1}{n_o^2} - r_{63} E_3 \right) + \eta^2 \left(\frac{1}{n_o^2} + r_{63} E_3 \right) + \frac{y^2}{n_e^2} = 1 \tag{1.63}$$

with

$$n_\zeta = n_o + \frac{1}{2} n_o^3 r_{63} E_3 \tag{1.64}$$

$$n_\eta = n_o - \frac{1}{2} n_o^3 r_{63} E \tag{1.65}$$

$$n_y = n_e \tag{1.66}$$

1.5.5 Bismuth Tellurium Oxide-Bi_2TeO_5 (BTeO)

This one is a photovoltaic crystal (see Section 2.4.1.2.1) with $\alpha = 5\ \text{cm}^{-1}$ at $\lambda = 532$ nm [12] and $\epsilon = 70$ [13].

1.6 Concluding Remarks

The aim of this chapter was just to recall some fundamental properties of optically anisotropic materials and the way an electric field is able to modify the index ellipsoid via an electro-optic effect. We have briefly shown how to calculate these effects in a few kinds of crystal having different electro-optic tensors. We hope these examples will enable the reader to understand how to operate on different materials, different crystals and different optical configurations.